Synthesis and in vitro evaluation of dioxopyrrolopyrroles as potential low-affinity fluorescent Ca^{2+} indicators

Nesibe Avcıbaşı,[1,2] Mario Smet,[1] Bert Metten,[1] Wim Dehaen,[1,†] Frans C. De Schryver,[1] Geert Bultynck,[3] Geert Callewaert,[3] Humbert De Smedt,[3] Ludwig Missiaen,[3] and Noël Boens[1,‡]

[1] *Department of Chemistry, Katholieke Universiteit Leuven, Celestijnenlaan 200F, 3001 Heverlee, Belgium*

[2] *Department of Chemistry, Faculty of Science, Ege University, 35100 Bornova, Izmir, Turkey*

[3] *Laboratory of Physiology, Katholieke Universiteit Leuven, Campus Gasthuisberg O & N, Herestraat 49, 3001 Heverlee, Belgium*

ABSTRACT. Three new low-affinity fluorescent Ca^{2+} indicators excitable with visible light, namely 3-phenyl-6-(4-(3-carboxymethoxy-4-(N,N-dicarboxymethylamino)phenyl)phenyl)-2,5-dicarboxymethyl-1,4-dihydropyrrolo[3,4-*c*]pyrrole-1,4-dione (DPP1), 3-phenyl-6-(5-(3-carboxymethoxy-4-(N,N-dicarboxymethylamino)phenyl)thien-2-yl)-2,5-dicarboxymethyl-1,4-dihydropyrrolo[3,4-*c*]pyrrole-1,4-dione (DPP2) and 3-(thien-2-yl)-6-(5-(3-carboxymethoxy-4-(N,N-dicarboxymethylamino)phenyl)thien-2-yl)-2,5-dicarboxymethyl-1,4-dihydropyrrolo[3,4-*c*]pyrrole-1,4-dione (DPP3) have been synthesized and evaluated for their Ca^{2+} binding properties via fluorimetric titrations. The in vitro dissociation constant K_d measured at 21 °C in 100 mM KCl buffered solution, pH 7.05, for the Ca^{2+}–DPP1 complex is 10 μM; for Ca^{2+}–DPP2 and Ca^{2+}–DPP3 a K_d value of 20 μM is found. All three indicators form 1 : 1 complexes with Ca^{2+}. The fluorescence quantum yields of the uncomplexed forms of DPP1, DPP2 and DPP3 are 1.2×10^{-2}, 3.4×10^{-2} and 3.6×10^{-2}, respectively. After binding to Ca^{2+} these values increase to 4.8×10^{-2}, 5.0×10^{-2} and 5.1×10^{-2}, respectively.

1. INTRODUCTION

From a functional point of view Ca^{2+} is probably the most important intracellular ion. Measurements of (changes in) cytosolic free Ca^{2+} concentrations with fluorescent probes have enabled scientists to investigate the role of Ca^{2+} in numerous physiological processes. The development of fluorescent indicators, with APTRA (*o*-aminophenol-*N*,*N*,*O*-triacetic acid) [1] and BAPTA [1,2-bis(*o*-aminophenoxy)ethane-N,N,N',N'-tetraacetic acid) [2] moieties as Ca^{2+} chelators and showing shifts in their excitation and/or emission spectra upon binding Ca^{2+}, entailed a major breakthrough in the elucidation of intracellular Ca^{2+} dynamics [3]. Cells at rest have a cytosolic free Ca^{2+} concentration of around 100 nM; upon activation, this level can rise to well above 1 μM. These changes play a pivotal role in many cellular processes, ranging from muscle contraction, neuronal signaling, secretion, fertilization, cell division, to metabolism and cell death [4]. Although intracellular Ca^{2+} levels are at least in resting conditions, below 1 μM, the increase in Ca^{2+} is expected to be much higher in close proximity of the mouth of the Ca^{2+} channels. Moreover, the level of the luminal Ca^{2+} concentration in the cellular organelles may be very important for controlling Ca^{2+} release from intracellular stores as well as Ca^{2+} entry from the outside medium. Low-affinity Ca^{2+} indicators—with Ca^{2+} dissociation constants above 1 μM—have therefore been used to measure elevated intracellular Ca^{2+} levels [5] and for Ca^{2+} concentration measurements in the lumen of stores [6]. Ca^{2+} levels around and above 1 μM saturate the response of the most frequently used Ca^{2+} probes based on the tetracarboxylate Ca^{2+} ligand BAPTA [2]. Low-affinity indicators generally use the tricarboxylate chelator APTRA with low affinity for Ca^{2+} (ground-state dissociation constant K_d for the Ca^{2+}–APTRA complex is around 30 μM) [1].

In this study we have developed three new fluorescent indicators with low affinity for Ca^{2+}, consisting of the chelator APTRA linked to a fluorescent dioxopyrrolopyrrole moiety. The new indicators are 3-phenyl-6-(4-(3-carboxymethoxy-4-(N,N-dicarboxymethylamino)phenyl)phenyl)-2,5-dicarboxymethyl-1,4-dihydropyrrolo[3,4-*c*]pyrrole-1,4-dione (DPP1), 3-phenyl-6-(5-(3-carboxymethoxy-4-(N,N-dicarboxymethylamino)phenyl)thien-2-yl)-2,5-dicarboxymethyl-1,4-dihydropyrrolo[3,4-*c*]pyrrole-1,4-dione (DPP2) and 3-(thien-2-yl)-6-(5-(3-carboxymethoxy-4-(N,N-dicarboxymethylamino)phenyl)thien-2-yl)-2,5-dicarboxymethyl-1,4-dihydropyrrolo[3,4-*c*]pyrrole-1,4-dione (DPP3). Their chemical structures are shown in Figure 1.

†E-mail: Wim.Dehaen@chem.kuleuven.ac.be
‡E-mail: Noel.Boens@chem.kuleuven.ac.be

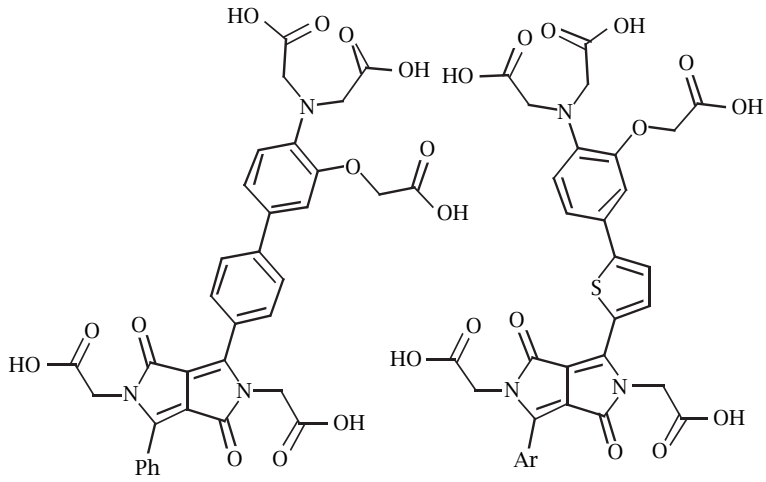

DPP1

DPP2 Ar = phenyl
DPP3 Ar = 2-thienyl

Figure 1. *Structures of DPP*1*, DPP2 and DPP*3*.*

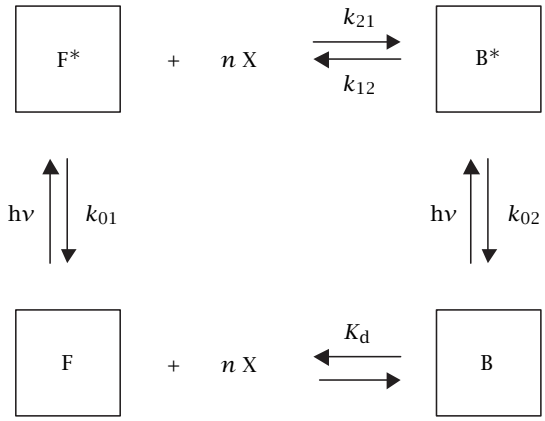

Scheme 1. *Kinetic scheme of the ground and excited-state association–dissociation between fluorescent indicator and cation.*

In addition to the synthesis of DPP1, DPP2 and DPP3, we also report their spectroscopic and Ca^{2+} binding properties in aqueous solution.

2. DETERMINATION OF K_d FROM DIRECT FLUORIMETRIC TITRATION

In a previous paper [7] we have derived the expression of the fluorescence signal F as a function of the cation concentration for the case of an n : 1 complex between a fluorescent indicator and a cation (n denotes the stoichiometry of the formed complex, Scheme 1).

Consider a photophysical system consisting of the free (uncomplexed) form of the indicator (F) which in the ground state can undergo a reversible association with cation X to form an n : 1 ion–indicator complex [i.e., the bound form (B) of the indicator]. Assuming an n : 1 stoichiometry between X and F, the association–dissociation can be described by the ground-state dissociation constant K_d [eq. (1)],

$$K_d = [F][X]^n/[B] \quad (1)$$

in which [ ] denote molarities. It should be noted that Scheme 1 depicts only the overall association–dissociation between an indicator and a cation [7], so that K_d represents the overall dissociation constant. In Scheme 1, it is further assumed that only species F and B absorb light at the excitation wavelength λ_{ex} to create the corresponding excited-state species F* and B*, which can decay by fluorescence (F) and non-radiative (NR) processes. The composite rate constant for deactivation of species F* is denoted by $k_{01}(= k_{F1} + k_{NR1})$ and by k_{02} for species B*. The overall rate constant describing the association F* + nX → B* is denoted by k_{21}, while the overall rate constant for the dissociation of B* into F* and nX is represented by k_{12}.

If the system depicted in Scheme 1 is excited with light of constant intensity, and if the absorbance of the same sample is sufficiently low (< 0.1), and moreover, if one assumes that the intermediate complexes (between F and one or more cations) are present in concentration low enough to give only a negligible contribution to the total fluorescence intensity, and that the rate of cation binding in the excited state can be neglected, then the

total fluorescence signal $F(\lambda_{ex}, \lambda_{em}, [X])$ at cation concentration [X], due to excitation at λ_{ex} and observed at emission wavelength λ_{em} can be expressed by eq. (2) [7]

$$F(\lambda_{ex}, \lambda_{em}, [X]) = \frac{[X]^n F_{max} + K_d F_{min}}{K_d + [X]^n} \qquad (2)$$

where F_{min} represents the fluorescence signal of the uncomplexed form F* of the indicator and F_{max} denotes the fluorescence signal of the bound form B*. F_{min} and F_{max} thus correspond to fluorescence signals at minimum and maximum X concentration. Fitting eq. (2) to the fluorescence data F as a function of [X] yields values for K_d, n, F_{min} and F_{max}.

3. RESULTS AND DISCUSSION

3.1. Indicator design. 1,4-Dioxo-3,6-diphenylpyrrolo[3,4-*c*]pyrrole (DPP) and variously substituted analogues comprise a relatively new class of red pigments that usually display excellent photostability and a high quantum yield of fluorescence [8, 9]. Among the desired properties of fluorescent indicators for intracellular cations are high molar extinction coefficients, a high quantum yield of fluorescence, the ability to use visible light excitation to reduce the risk of cellular photodamage and the interference of cellular autofluorescence, and good chemical as well as photochemical stability. As DPP derivatives usually display these qualities, we designed and synthesized the indicators DPP1, DPP2 and DPP3 with dioxopyrrolopyrrole as fluorophore.

For the measurement of elevated free Ca^{2+} concentrations (above 1 μM) a low-affinity chelator of Ca^{2+} is required. Therefore, we choose as Ca^{2+} complexing moiety a derivative of APTRA [1].

3.2. Synthesis of the indicators. In general, the new indicators are synthesized by Stille coupling (Schemes 3 and 4) between the tin derivatives of the respective dioxopyrrolopyrroles and the brominated *t*-butyl triester **6** of APTRA (Scheme 2). To synthesize DPP1, bromophenyl derivative **7** (Scheme 3, gift from Dr. O. Wallquist of Ciba Specialty Chemicals) was used as starting material. For DPP2, dithienyl derivative **3b** was synthesized as starting material by a literature procedure [8], namely the base catalyzed condensation of two equivalents of thiophene-2-carbonitrile (**2**) with diethyl succinate (Scheme 2). When a 5 : 1 mixture of benzonitrile (**1**) and thiophene-2-carbonitrile (**2**) was used under the same conditions (Scheme 2), a maximum yield of the mixed DPP **3a** was obtained, reflecting the higher reactivity of the thiophene carbonitrile. Of course, this condensation also yields two undesired symmetrically substituted analogues. To remove these, the mixture was treated with Boc_2O, yielding a mixture of the respective diBoc-derivatives which were separated by column chromatography. After separation, the symmetrical derivatives were discarded whereas the desired asymmetrically substituted diBoc-derivative **4** was converted back into **3a** by straightforward reflux in methoxyethanol (as this is a polar solvent in which **3a** is only slightly soluble, it allows the isolation of **3a** by filtration). Compound **3a** serves as the starting material for the synthesis of DPP3. Since direct bromination of the *t*-butyl triester of APTRA was anticipated to be problematic, bromide **6** was prepared by alkylation of 4-bromo-2-hydroxyaniline (**5**) [10] with *t*-butyl bromoacetate (Scheme 2). We found that the use of Huenig's base (diisopropylethylamine) was the best way to avoid cyclization.

For the synthesis of DPP1, bromophenyl-DPP **7** was transformed into the diacetate **8** by direct alkylation with *t*-butyl bromoacetate (Scheme 3). In general, the solubility in organic solvents of acetates such as **8** dramatically increased with respect to the initial DPPs which are usually highly insoluble. Moreover, the introduction of these acetate esters allows final conversion into acetate salts, which will assure water solubility of the target compounds, under the same conditions as for the deprotection of the APTRA residue. Diacetate **8** could readily be transformed into the tin derivative **9** by treatment with hexakisbutylditin in the presence of $Pd(PPh_3)_4$. Finally, tin derivative **9** could be coupled with the bromo-APTRA ester **6** under classical Stille conditions, yielding the conjugate **10** which displayed excellent solubility in organic solvents such as dichloromethane and acetone. Finally, the desired indicator DPP1 was obtained by deprotection of the five *t*-butyl ester groups with trifluoroacetic acid. This compound was found to be sufficiently soluble in water for fluorimetric measurements.

Tin compounds **11a** and **11b** were obtained directly from the unsubstituted derivatives **3a** and **3b** in a one pot procedure (Scheme 4). Thus, the initial DPP was treated with an excess of LDA, resulting in the deprotonation of the nitrogen atoms and of the free alpha position of the thiophene substituent. Addition of tributyltin chloride then resulted in stannylation of the latter thienyl carbanion. Finally, addition of *t*-butyl bromoacetate and heating resulted in the alkylation of the free nitrogen atoms as well, yielding **11a** and **11b** which both are highly soluble in common organic solvents. Coupling of these two tin derivatives with bromo-APTRA derivative **6** in the presence of $Pd(PPh_3)_4$ yielded the conjugates **12a** and **12b** and subsequent deprotection with trifluoroacetic acid gave rise to the two desired indicators DPP2 and DPP3.

3.3. Excitation and emission spectra. The interaction of the three DPP indicators with Ca^{2+} can be followed by fluorescence spectroscopy. The changes in the fluorescence excitation and emission spectra of the three probes that accompany Ca^{2+} complexation (from 0 to 0.95 mM free Ca^{2+}) are illustrated in Figure 2. For DPP1, excitation spectra were recorded at

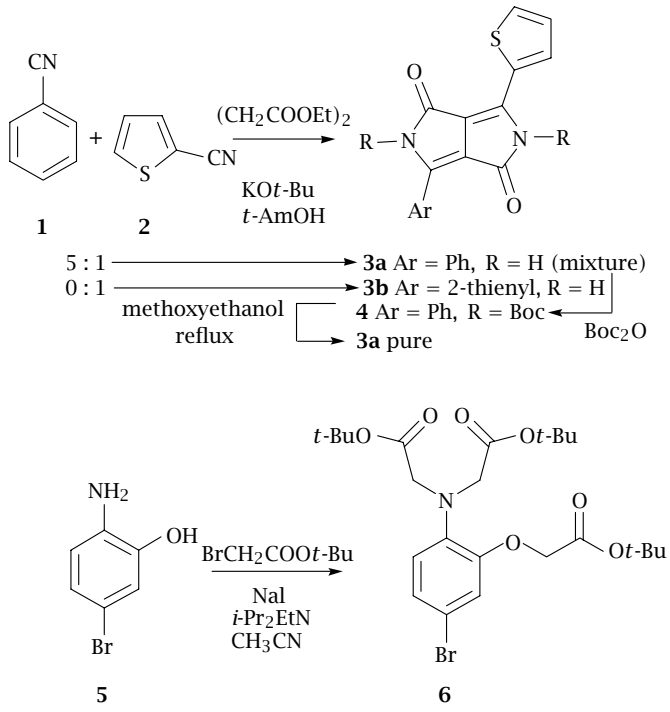

Scheme 2.

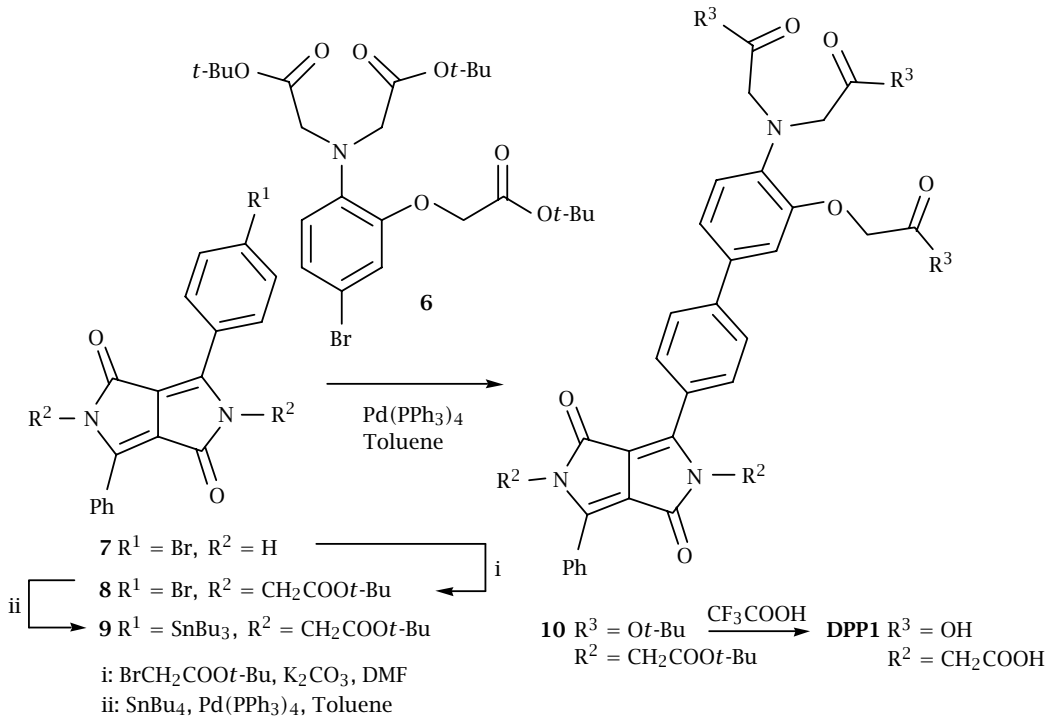

Scheme 3. *Synthesis of DPP*1.

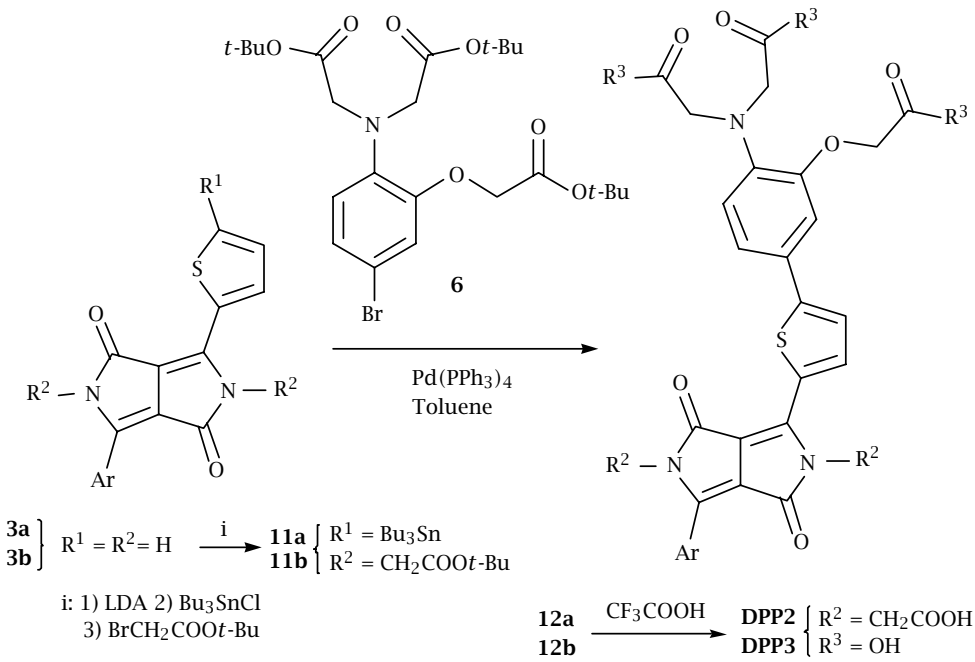

Scheme 4. *Synthesis of DPP2 and DPP3.*

the observation wavelengths of 520, 530 (Figure 2A), 540 and 545 nm. All spectra show a rather broad band with some structure and with two maxima of approximately equal intensity at 464 and 475 nm. The associated emission spectra—obtained at λ_{ex} = 460, 470, 480 and 490 (Figure 2D) nm—also display a broad band with a maximum at 538 nm and a shoulder at 566 nm. Fluorescence excitation spectra of DPP2 were scanned while monitoring the emission at 590 (Figure 2B), 600 and 640 nm. Its emission spectra were measured upon excitation at 519 (Figure 2E), 526, 533 and 540 nm. The excitation spectra show a broad structureless band with a maximum at 520 nm. The emission spectra reach their maximum intensity at 600 nm with an additional shoulder at 645 nm. Excitation spectra of DPP3 were scanned while following the emission at 580, 590 (Figure 2C), 600, 610 and 640 nm, whereas the emission spectra were recorded upon excitation at λ_{ex} = 540, 550, 560 (Figure 2F), and 570 nm. The excitation spectra show two maxima: in the absence of Ca^{2+} the major maximum is at 528 nm with a minor maximum at 561 nm. Upon increasing the free Ca^{2+} concentration, the intensity at 561 nm increases relatively more than at 528 nm, so that at high Ca^{2+} levels the major maximum is at 561 while the minor maximum is at 528 nm. The emission spectra show two intensity maxima: at 611 and 650 nm. Without Ca^{2+} the major maximum is located at 650 nm; upon increasing the Ca^{2+} concentration the band at 611 nm grows relatively more to become the major one when DPP3 is saturated with Ca^{2+}. It is clear that for all DPP indicators Ca^{2+} complexation causes an increase in fluorescence intensity without any significant spectral shift. The spectroscopic properties of DPP1, DPP2 and DPP3 at pH 7.05 are summarized in Table 1.

The fluorescence intensity increases upon binding Ca^{2+} (as illustrated Figure 2) indicate a higher fluorescence quantum yield, Φ_f, of the Ca^{2+} bound form of the indicators than of the uncomplexed form. This is indeed what is found (see Table 1). The increase is more pronounced for DPP1 (approximately 4-fold) than for DPP2 and DPP3 (both about 1.5-fold). The low fluorescence quantum yields necessitate high indicator loading levels. Table 1 also compiles the values of Φ_f and the molar extinction coefficients ε of the three probes.

3.4. Cation binding properties. By following the increase of fluorescence intensity in the excitation spectra (Figure 3) with higher [Ca^{2+}], K_d and the stoichiometry n of the complexes of DPP1, DPP2 and DPP3 with Ca^{2+} can be estimated by non-linear fitting of eq. (2) to the fluorimetric titration data. Least-squares estimation with all parameters (K_d, n, F_{min} and F_{max}) freely adjustable usually gave unacceptable fits with parameter estimates with extremely large standard deviations. Moreover, the F_{min} and F_{max} estimates were very different from the experimental fluorescence intensities obtained at zero and high [Ca^{2+}], respectively. Therefore, we decided to keep F_{min} and F_{max} fixed at the measured fluorescence intensities at zero and maximum Ca^{2+} concentration, respectively, during the fitting procedure. Since all estimated stoichiometry values n were indicative of a 1 : 1 complex between indicator and Ca^{2+}, we further held n constant (at unity) in the

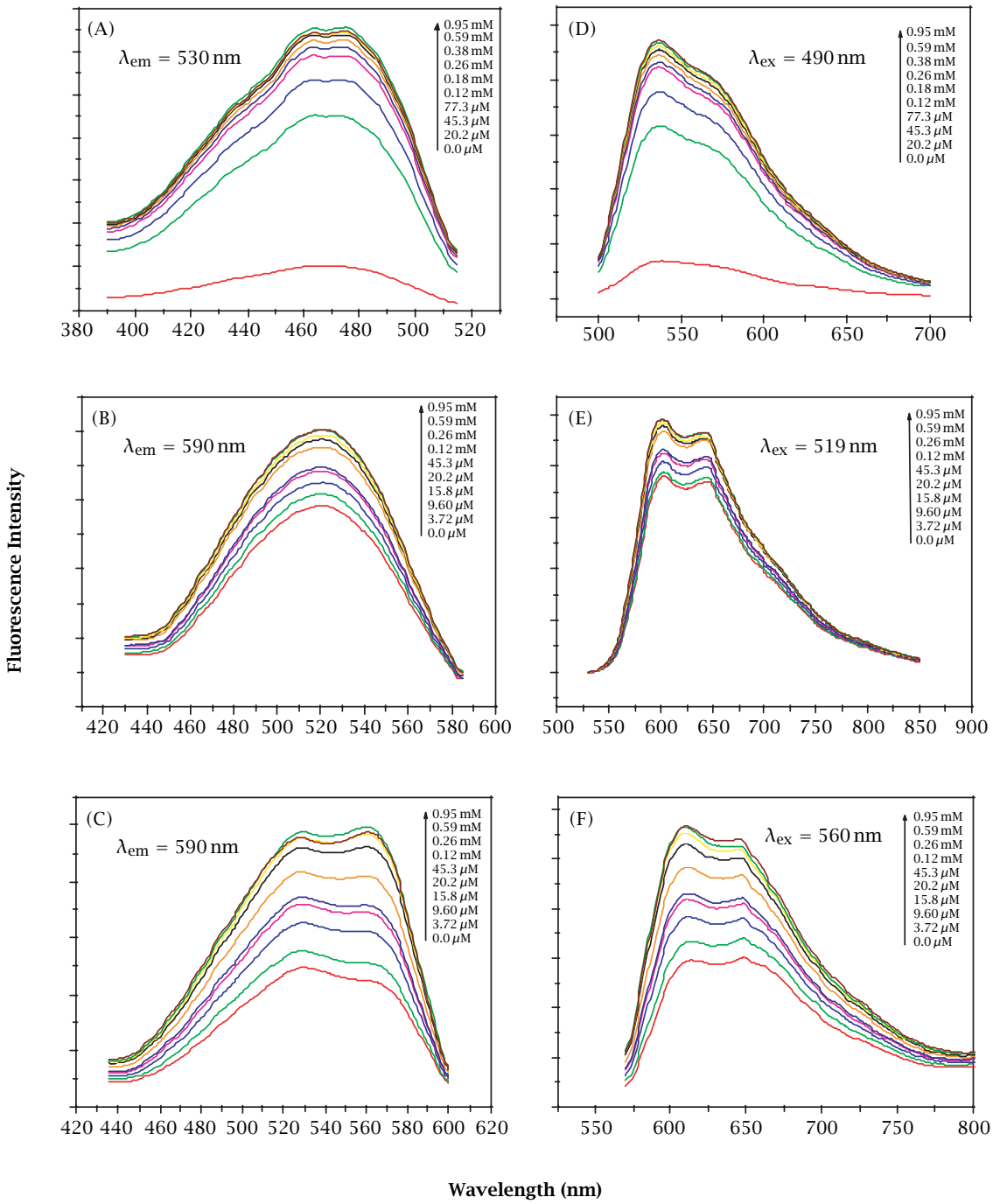

Figure 2. *Fluorescence excitation spectra of DPP*1 *(A), DPP*2 *(B) and DPP*3 *(C) in buffered solutions containing zero to* 0.95 mM Ca^{2+}. *Corresponding fluorescence emission spectra of DPP*1 *(D), DPP*2 *(E) and DPP*3 *(F) as a function of* [Ca^{2+}]. *All spectra were recorded at* 21 °C *using solutions containing* 100 mM KCl *and* 10 mM *MOPS, pH* 7.05.

subsequent parameter estimation (i.e., only K_d is an adjustable parameter). For DPP2 and DPP3 unacceptable fits were obtained with very large standard deviations for K_d when n was adjustable. The estimated K_d (and n) values for the Ca^{2+} complexes with the three indicators are compiled in Table 2. Some illustrative examples of the non-linear least-squares fitting of eq. (2) to the fluorimetric titration data as a function of free [Ca^{2+}] are shown in Figure 3.

The estimated K_d values are in the range of elevated intracellular [Ca^{2+}]. The average K_d values at 21 °C in 100 mM KCl, pH 7.05, computed from the K_d estimates

Table 1. *Spectroscopic properties of DPP*1, *DPP*2 *and DPP*3 *in uncomplexed (free) and* Ca^{2+} *bound forms, determined at pH* 7.05 *and* 21 °C *in solutions containing* 10 mM *MOPS and* 100 mM KCl.

Compound	Excitation λ_{max} (nm)		Emission λ_{max} (nm)		Φ_f		λ^{ex} Reference	$\Phi_{reference}$	ε	
	free	bound	free	bound	free	bound			free	bound
DPP1	464, 475	464, 475	538	538	1.1×10^{-2}	4.5×10^{-2}	470 nm-fluorescein in 0.1 N NaOH	0.90	12900±50	12930±30
			sh 566	sh 566	1.3×10^{-2}	5.1×10^{-2}	470 nm-rhodamin 6G in H_2O	0.76		
DPP2	520	520	600	600	3.4×10^{-2}	5.0×10^{-2}	526 nm-rhodamin 6G in H_2O	0.81	14500±300	14260±80
			sh 645	sh 645						
DPP3	528	561	650	611	3.9×10^{-2}	5.3×10^{-2}	555 nm-cresyl violet perchlorate in EtOH	0.50	37000±1000	25000±1000
	sh 561	sh 528	sh 611	sh 650	3.3×10^{-2}	4.9×10^{-2}	568 nm-cresyl violet perchlorate in EtOH	0.51		

Table 2. *Non-linear least-squares estimation [eq.* (2)*] of* K_d *and* n *for the* Ca^{2+}*-DPP*1, Ca^{2+}*-DPP*2 *and* Ca^{2+}*-DPP*3 *complexes by direct fluorimetric titration.* F_{min} *and* F_{max} *were kept fixed during all fittings.*

Compound	Experimental excitation and emission wavelength (nm)		K_d (μM)	n
DPP1	λ_{ex} = 480 nm	λ_{em} = 535 nm	5 ± 3[a]	1.08 ± 0.04
	λ_{ex} = 480 nm	λ_{em} = 535 nm	10 ± 0.4[a]	1[c]
	λ_{ex} = 436 nm	λ_{em} = 530 nm	4 ± 2[b]	1.11 ± 0.04
	λ_{ex} = 436 nm	λ_{em} = 530 nm	10 ± 0.4[b]	1[c]
	λ_{ex} = 470 nm	λ_{em} = 530 nm	5 ± 2[b]	1.09 ± 0.04
	λ_{ex} = 470 nm	λ_{em} = 530 nm	10 ± 0.4[b]	1[c]
	λ_{ex} = 470 nm	λ_{em} = 537 nm	7 ± 3[b]	1.05 ± 0.04
	λ_{ex} = 470 nm	λ_{em} = 537 nm	10 ± 0.3[b]	1[c]
	λ_{ex} = 463 nm	λ_{em} = 537 nm	9 ± 3[b]	1.03 ± 0.04
	λ_{ex} = 463 nm	λ_{em} = 537 nm	10 ± 0.3[b]	1[c]
DDP2	λ_{ex} = 540 nm	λ_{em} = 644 nm	100 ± 300[a]	0.8 ± 0.2
	λ_{ex} = 540 nm	λ_{em} = 644 nm	20 ± 5[a]	1[c]
	λ_{ex} = 540 nm	λ_{em} = 603 nm	100 ± 300[a]	0.8 ± 0.2
	λ_{ex} = 540 nm	λ_{em} = 603 nm	20 ± 5[a]	1[c]
	λ_{ex} = 515 nm	λ_{em} = 600 nm	200 ± 400[b]	0.8 ± 0.2
	λ_{ex} = 515 nm	λ_{em} = 600 nm	20 ± 4[b]	1[c]
DDP3	λ_{ex} = 560 nm	λ_{em} = 644 nm	500 ± 900[a]	0.7 ± 0.2
	λ_{ex} = 560 nm	λ_{em} = 644 nm	20 ± 5[a]	1[c]
	λ_{ex} = 560 nm	λ_{em} = 619 nm	300 ± 600[a]	0.7 ± 0.2
	λ_{ex} = 560 nm	λ_{em} = 619 nm	20 ± 5[a]	1[c]
	λ_{ex} = 563 nm	λ_{em} = 590 nm	100 ± 300[b]	0.8 ± 0.2
	λ_{ex} = 563 nm	λ_{em} = 590 nm	20 ± 5[b]	1[c]
	λ_{ex} = 519 nm	λ_{em} = 590 nm	200 ± 500[b]	0.7 ± 0.2
	λ_{ex} = 519 nm	λ_{em} = 590 nm	20 ± 5[b]	1[c]
	λ_{ex} = 523 nm	λ_{em} = 610 nm	200 ± 500[b]	0.8 ± 0.2
	λ_{ex} = 523 nm	λ_{em} = 610 nm	20 ± 5[b]	1[c]
	λ_{ex} = 564 nm	λ_{em} = 610 nm	200 ± 400[b]	0.8 ± 0.2
	λ_{ex} = 564 nm	λ_{em} = 610 nm	20 ± 5[b]	1[c]

[a] Determined by monitoring the increase of the fluorescence emission signal upon addition of Ca^{2+}.
[b] Determined by monitoring the increase of the fluorescence excitation signal upon addition of Ca^{2+}.
[c] n kept constant.

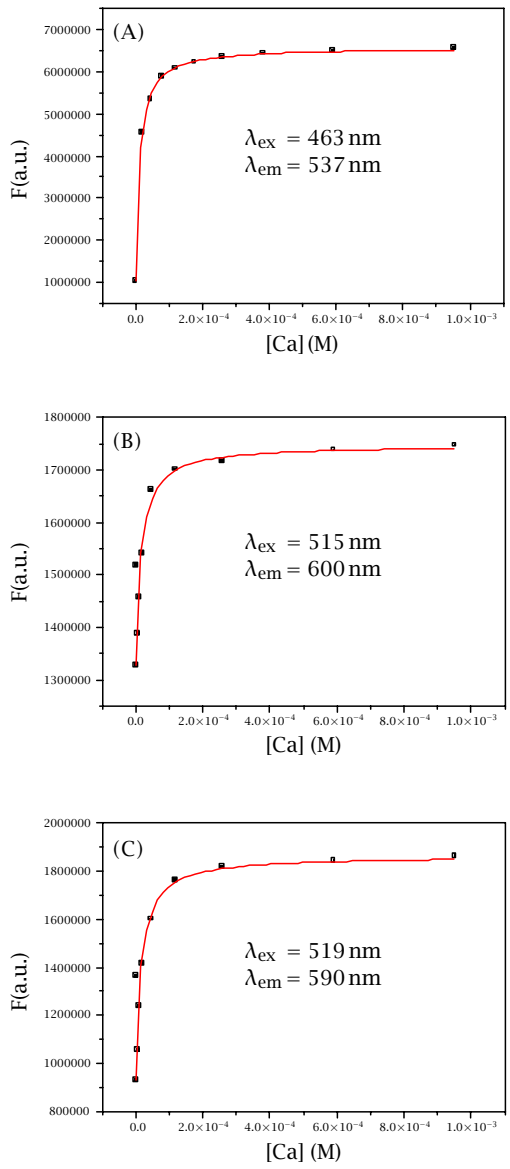

Figure 3. *Estimation of K_d and n for* Ca^{2+}*–DPP*1, Ca^{2+}*–DPP*2 *and* Ca^{2+}*–DPP*3 *complexes using direct fluorimetric titration [eq.* (2)*; A, B and C, respectively]. For DPP*2 *and DPP*3*, n was kept constant at unity during the fitting. Data were obtained from experiments performed at* 21 °C *and pH* 7.05 *(see Table 2).*

with $n = 1$ for Ca^{2+}–DPP1, Ca^{2+}–DPP2 and Ca^{2+}–DPP3 are 10 μM, 20 μM and 20 μM, respectively.

4. CONCLUSIONS

Three new fluorescent indicators with a low affinity for Ca^{2+} (DPP1, DPP2 and DPP3, Figure 1) have been designed and synthesized. The new indicators are excitable with visible light and have dissociation constants for Ca^{2+} in the micromolar range, so that they are suitable to detect elevated intracellular Ca^{2+} levels. The low fluorescence quantum yield values (only a few percent) of the uncomplexed as well as of the Ca^{2+} bound forms require high loading indicator concentrations. The absence of any significant spectral shift in the excitation and emission spectra makes the new indicators non-ratiometric.

5. EXPERIMENTAL SECTION

5.1. Materials and methods. THF was dried by distillation from sodium/benzophenone. All other reagents and solvents were purchased from Acros Organics and used without further purification. Mass spectra were recorded on a Perkin Elmer instrument (EI 70 eV or ES). ^{1}H-NMR and ^{13}C-NMR spectra were recorded on a Bruker AMX 400 MHz or Bruker Avance 300 MHz. The absorption measurements were performed on a Perkin Elmer Lambda 40 UV/VIS spectrometer. Up to six probe concentrations were used for the determination of the molar extinction coefficients, ε, of each probe.

5.2. Steady-state fluorescence. Corrected steady-state excitation and emission spectra were recorded on a SPEX Fluorolog-3. The fluorimetric measurements were done on solutions made up to mimic the intracellular milieu of mammalian cells. The solutions contained 100 mM KCl and 10 mM MOPS (3-[*N*-morpholino]propanesulfonic acid), and were adjusted to pH 7.05 with KOH or HCl. The free Ca^{2+} concentration in the solutions was adjusted with Ca^{2+}–nitrilotriacetic acid buffers, as described by Fabiato and Fabiato [11]. Free Ca^{2+} concentrations were computed with the CHELATOR program developed by Schoenmakers et al. [12]. The indicator concentrations were 14.3 μM, yielding an absorbance per cm path length of approximately 0.1 at the absorption maximum.

Fluorescence quantum yields of the free and bound forms of indicators were determined using fluorescein in 0.1 N NaOH, rhodamin 6G in water, and cresyl violet perchlorate in ethanol as reference. The fluorescence quantum yields of these references were taken to be 0.90 for fluorescein, 0.76 (λ_{ex} = 488 nm) and 0.81 (λ_{ex} = 546 nm) for rhodamin 6G, and 0.50 (λ_{ex} = 546 nm) and 0.51 (λ_{ex} = 578 nm) for cresyl violet perchlorate [13]. The buffered (pH 7.05) solutions of the uncomplexed form of the indicator contained 100 mM KCl, 10 mM MOPS and 15 mM nitrilotriacetic acid. The buffered (pH 7.05) solutions of the Ca^{2+} bound form were made up of 0.95 mM free Ca^{2+}, 100 mM KCl and 10 mM MOPS. The indicator concentration was chosen so that the absorbance at the excitation wavelength never exceeded 0.1. All aqueous solutions were prepared with Milli-Q water. All measurements were done at 21 °C.

6. SYNTHESIS

A detailed description of the synthesis is available electronically as supplementary material.

ACKNOWLEDGMENTS

Dr. O. Wallquist (Ciba Specialty Chemicals) is gratefully acknowledged for kindly supplying us with a sample of brominated DPP. N.A. wishes to thank Prof. Dr. S. Icli for his support. M.S. and G.B. are postdoctoral fellows of the *Fonds voor Wetenschappelijk Onderzoek - Vlaanderen* (FWO). The authors are grateful to the University Research Fund of the K. U. Leuven for IDO-grant IDO/00/001 and to the FWO for grant G.0320.00. The DWTC (Belgium) through IAP-V-03 is thanked for continuing support.

REFERENCES

[1] P. A. Otten, R. E. London, and L. A. Levy, Bioconjug. Chem. **12** (2001), 76.

[2] R. Y. Tsien, Biochemistry **19** (1980), 2396.

[3] R. Y. Tsien, Annu. Rev. Neurosci. **12** (1989), 227; W. J. J. M. Scheenen, A. M. Hofer, and T. Pozzan, in Cell Biology: A Laboratory Handbook, Vol. 3, 2nd Ed., (J. E. Celis, Ed.), Academic Press, 1998, p. 363; A. Takahashi, P. Camacho, J. D. Lechleiter, and B. Herman, Physiol. Rev. **79** (1999), 1089.

[4] M. J. Berridge, M. D. Bootman, and P. Lipp, Nature **395** (1998), 645; M. J. Berridge, P. Lipp, and M. D. Bootman, Nature Rev. Mol. Cell Biol. **1** (2000), 11; M. J. Berridge, Cell Calcium **32** (2002), 235.

[5] I. Parker, J. Choi, and Y. Yao, Cell Calcium **20** (1996), 105; J. Eilers, G. Callewaert, C. Armstrong, and A. Konnerth, Proc. Natl. Acad. Sci. USA **92** (1995), 10272; S. Rajdev and I. J. Reynolds, Neurosci. Lett. **162** (1993), 149; M. Konishi, S. Hollingworth, A. B. Harkins, and S. M. Baylor, J. Gen. Physiol. **97** (1991), 271; M. Zhao, S. Hollingworth, and S. M. Baylor, Biophys. J. **70** (1996), 896.

[6] K. Hirose and M. Iino, Nature **372** (1994), 791; F. H. Van de Put, J. J. De Pont, and P. H. Willems, J. Biol. Chem. **269** (1994), 12438; T. Sugiyama and W. F. Goldman, Am. J. Physiol. **269** (1995), C698; M. Zhao, S. Hollingworth, and S. M. Baylor, Biophys. J. **70** (1996), 896; M. P. Blaustein and V. A. Golovina, Science **275** (1997), 1643.

[7] E. Cielen, A. Stobiecka, A. Tahri, G. J. Hoornaert, F. C. De Schryver, J. Gallay, M. Vincent, and N. Boens, J. Chem. Soc., Perkin Trans. **2** (2002), 1197.

[8] A. Iqbal, M. Jost, R. Kirchmayr, J. Pfenninger, A. Rochat, and O. Wallquist, Bull. Soc. Chim. Belg. **97** (1988), 615; A. C. Rochat, L. Cassar, and A. Iqbal, Europ. Patent (1983), 0094911.

[9] A. Iqbal, L. Cassar, A. C. Rochat, J. Pfenninger, and O. Wallquist, J. Coat. Tech. **60** (1988), 37; J. Mizuguchi and A. C. Rochat, J. Imag. Sci. **32** (1988), 135; J. Mizuguchi, J. Appl. Phys. **66** (1989), 3111; J. Mizuguchi, A. C. Rochat, and G. Rihs, Ber. Bunsenges. Phys. Chem. **96** (1992), 607; J. Mizuguchi, Chimia **48** (1994), 439.

[10] H. Gershon, D. D. Clarke, and M. Gershon, Monatsh. Chem. **124** (1993), 367.

[11] A. Fabiato and F. Fabiato, J. Physiol. (Paris) **75** (1979), 463.

[12] T. J. M. Schoenmakers, G. J. Visser, G. Flik, and A. P. R. Theuvenet, Biotechniques **12** (1992), 870.

[13] J. Olmsted, J. Phys. Chem. **83** (1979), 2581.